

Enhancing Long-Range Exciton Guiding in Molecular Nanowires by H-Aggregation Lifetime Engineering

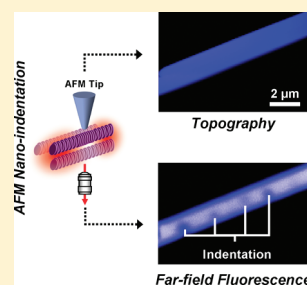
Debangshu Chaudhuri,^{*,†} Dongbo Li,[†] Yanke Che,[‡] Eyal Shafran,[†] Jordan M. Gerton,[†] Ling Zang,[‡] and John M. Lupton^{*,†}

[†]Department of Physics and Astronomy and [‡]Department of Materials Science and Engineering, University of Utah, Salt Lake City, Utah 84112, United States

S Supporting Information

ABSTRACT: Excitonic transitions in organic semiconductors are associated with large oscillator strength that limits the excited-state lifetime and can in turn impede long-range exciton migration. We present perylene-based emissive H-aggregate nanowires where the lowest energy state is only weakly coupled to the ground state, thus dramatically enhancing lifetime. Exciton migration occurs by thermally activated hopping, leading to luminescence quenching on topological wire defects. An atomic force microscope tip can introduce local topological quenchers by distorting the H-aggregate structure, demonstrating long-range exciton migration at room temperature and offering a potential route to writing fluorescent “nanobarcodes” and excitonic circuits.

KEYWORDS: H-aggregate, perylene bisimide, molecular wires, exciton migration, light harvesting, nanoindentation



Small molecules can order spontaneously in an ensemble to form crystalline structures with new optical properties that are controlled both by individual building blocks and by bulk assembly.^{1–3} Careful tuning of the shape and potential of molecular side groups allows the formation of anisotropic crystalline nanostructures^{1,2,4} such as fibers, wires and belts, which open applications as fluorescence quenching-based molecular sensors. The packing of the molecules sensitively controls the electronic properties of excitons formed by the coupling between individual monomers. This interaction lifts the degeneracy of energy levels of adjacent monomer units akin to the formation of symmetric and antisymmetric wave functions in two coupled quantum wells. Depending on the arrangement of the monomers, different coupling occurs. In J-aggregates, oscillator strength is transferred to the lower energy transition and in H-aggregates to the higher energy one.³ Consequently, only J-aggregates are strictly emissive with an accelerated radiative rate compared to the monomer building blocks and thus have been considered the spectroscopically more interesting class of molecular crystalline materials.^{5–7} However, H-aggregates support the molecular equivalent of an indirect exciton (i.e., dipole-forbidden by momentum selection rules) with a resulting increased excited-state lifetime⁸ that makes H-aggregates interesting for light-harvesting applications. While long-range migration of triplet excitons has been extensively studied in molecular crystals,⁹ we are not aware of similar studies for H-aggregate indirect excitons. In contrast, long-lived indirect excitons have been utilized in several inorganic materials to implement long-range (up to millimeters) migration of excitation energy,^{10,11} whereas the typical exciton diffusion lengths in (direct-exciton) molecular materials is on the nanometer scale.^{12–14} Only in the case of single defect-free

polydiacetylene chains, which have been shown to form perfect quantum wires, has evidence for thermally activated singlet exciton migration on macroscopic length scales been reported.¹⁵

Figure 1 summarizes the elementary optical properties of perylene tetracarboxylic diimide (PTCDI) and its anisotropic aggregates. A comparison of monomer and aggregate absorption spectra (reported in ref 16) reveals that the molecules form H-aggregates in the solid state with most of the monomeric oscillator strength being transferred from the monomers to the higher-lying transition (E_0-E_2 in panel a). The transition to the ground state (E_0) from the lower-energy excited state (E_1) is, however, not completely forbidden^{17–20} due to the rotational displacement of the monomers with respect to each other in the crystal;¹⁶ the molecules do not form a perfect H-aggregate, which would be entirely nonemissive. Panels b and c show photoluminescence (PL) spectra of the monomer (dispersed at a low concentration in a polystyrene film) and aggregate fibers at 300 and 4 K. The aggregate PL is red shifted by 0.37 eV with respect to the monomer, in agreement with the energy-level diagram in panel a. Lowering the temperature does not shift the mean transition energy but narrows the spectra (panel c), revealing the vibronic progression more clearly. Both monomer and aggregate have a similar vibronic substructure. The fact that vibronics are seen in the aggregate spectra is inconsistent with the common assignment of the spectrum to an excimer.^{17,19,20}

The emission properties of the nanowires are affected not only by the energetic splitting of the aggregate but also by the fact that

Received: September 17, 2010

Revised: November 5, 2010

Published: December 22, 2010

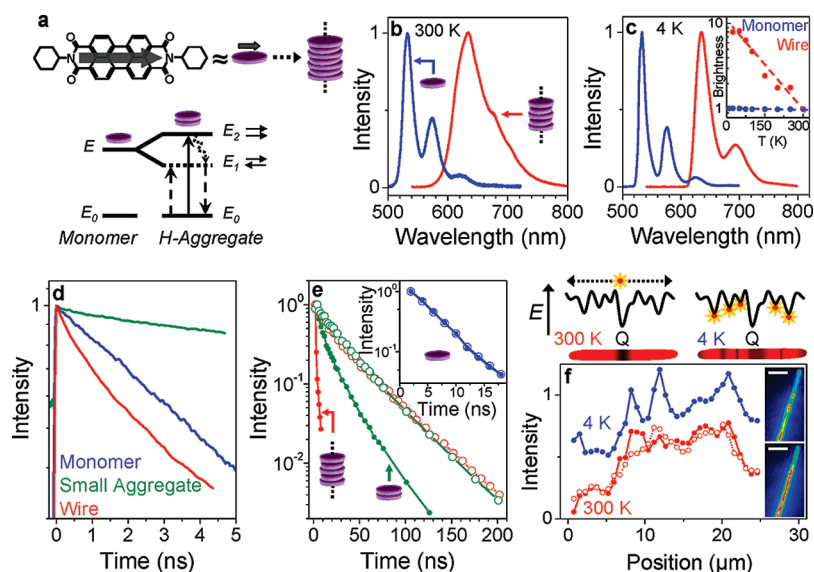


Figure 1. Luminescent H-aggregate perylene nanowires with thermally activated exciton migration and quenching. (a) Structure of the perylene tetracarboxylic diimide (PTCDI) monomer, which can stack in a disklike fashion to form highly ordered molecular crystal nanowires. The gray arrow indicates the transition dipole moment. Stacking of the monomers results in an H-aggregate with energy levels split between parallel and antiparallel dipole orientations. Most of the oscillator strength of the coupled dimer system is transferred to the higher-energy transition. Relaxation in the excited-state manifold necessitates emission from the lower-energy level, which is only weakly coupled to the ground state. (b) Emission of monomer and aggregates at 300 and 4 K (c). The monomer intensity does not depend on temperature, whereas the wire emission increases exponentially with decreasing temperature (inset). (d) Formation of the H-aggregate increases the PL lifetime (green) with respect to the monomer (blue), whereas larger aggregates (i.e., the nanowires) exhibit a reduction in lifetime (red). (e) Thermal activation of the PL lifetime. Small aggregates (green) and nanowires (red) have the same lifetime at 25 K (open circles) but differ at 300 K (closed circles). The excited-state lifetime of the monomer (inset) is independent of temperature. (f) Nonuniformity in wide-field single-wire PL due to local exciton quenching at defects in the nanowire. Because of local energetic disorder, at 300 K excitons can move further along the wire, leading to more overall quenching but weaker spatial modulation in intensity when compared to 4 K (cartoon). Intensity profiles of a wire under uniform excitation measured at 4 K (red) and 300 K (black), extracted from the microscope images to the right (scale bar 5 μm). The increase in spatial intensity modulation due to increased exciton localization at 4 K is reversible upon reheating the wire to 300 K (open symbols).

an exciton can move along the wire, where it may encounter a luminescence quenching site⁵ or become localized due to energetic disorder. Temperature controls exciton mobility in energetically disordered systems and thus has a large effect on the wire PL intensity³ (inset panel c). As the temperature is lowered from 300 to 4 K, the intensity increases exponentially by an order of magnitude, while the monomer PL yield remains constant. This rise in intensity is primarily due to a reduction in nonradiative decay, which is confirmed by considering the PL dynamics and the effect of aggregate size. Small aggregates of a few monomers can be formed by depositing films of PTCDI dispersed in polystyrene. These films appear uniform under the fluorescence microscope. Panel d compares the short-time PL dynamics of the monomer, small aggregates and nanowires as recorded with a streak camera at 300 K. As expected for an H-aggregate, the emission lifetime is increased (green line) with respect to the monomer (blue). However, we find that formation of a larger aggregate structure (red) reduces the PL lifetime. Panel e shows PL lifetime data of the monomer (inset) and the aggregates at 300 and 25 K. Whereas temperature has no effect on the monomer emission ($\tau_{\text{PL}} = 5$ ns), the wire PL lifetime is increased 27-fold upon cooling (from $\tau_{\text{PL}} = 1.7$ ns²¹ to $\tau_{\text{PL}} = 46$ ns). The wire PL lifetime is shorter than that of the monomer at room temperature, but much longer at lower temperatures. As the aggregate central PL peak does not change with temperature, we propose that it is the exciton dynamics that increase at elevated temperatures, leading to a reduction in PL yield and PL lifetime;

excitons become more mobile and tend to diffuse to quenching sites within the aggregate. As a consequence, the PL dynamics do not depend on aggregate size at low temperature, as seen in the comparison of small aggregates (green) and wires (red).

We note that temperature could also affect the crystal packing; increased molecular dynamics at elevated temperatures may weaken the H-aggregate structure. However, in this case we would expect to observe the opposite effect, that is, an independence of PL dynamics on aggregate size at higher temperatures.

In contrast to recent studies of J-aggregate nanowires,⁶ the H-aggregate wire luminescence is spatially nonuniform. As atomic force (AFM) and scanning-electron microscope studies reveal topographically flat structures,^{1,4,16} PL nonuniformities must originate from local variations in exciton quenching efficiency. Figure 1f shows PL images and intensity traces of the same wire recorded at 300 and 4 K. The trace of the reheated wire is also shown (open circles). The images indicate that the PL modulation contrast increases with decreasing temperature. Indeed, we confirmed this observation by computing the average PL modulation ΔI (see Supporting Information) along 20 different single wires at 300 and 4 K. ΔI was found to double upon cooling; as exciton migration is inhibited due to trapping in energetic minima³ along the wire, quenching becomes more local and intensity variations increase. The sketch illustrates the following interpretation: exciton localization in potential minima and quenching (Q) do not necessarily occur at the same position. At low temperatures, exciton diffusion to potential minima can lead to bright and dark regions. At room

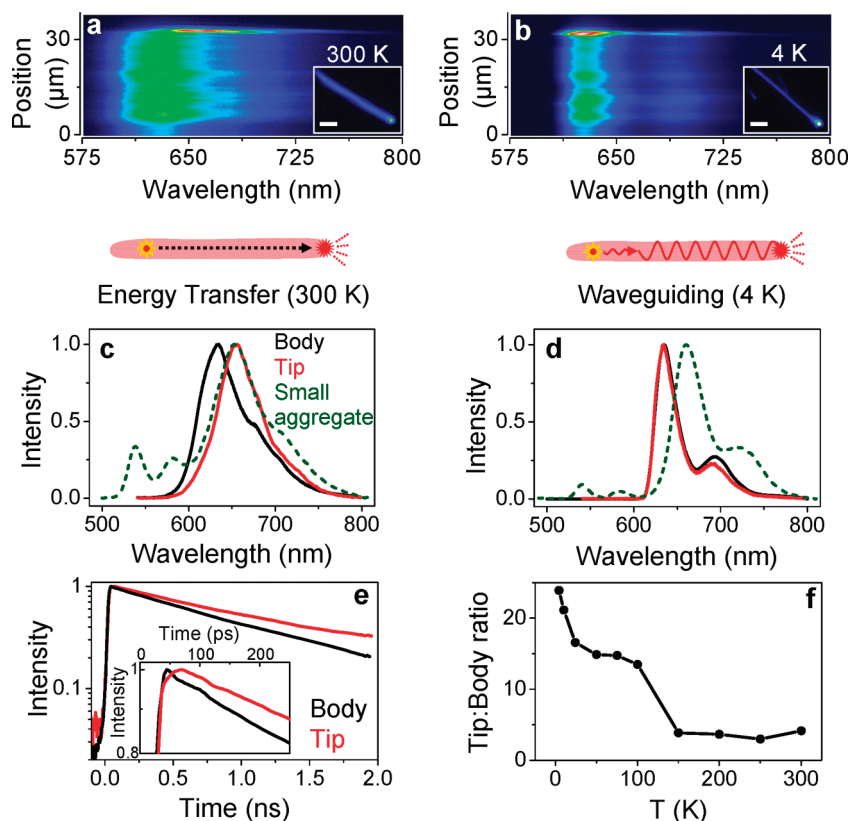


Figure 2. Exciton migration vs waveguiding in perylene nanowires under wide-field illumination. (a,b) Single wires generally show tip emission brighter than the bulk (scale bar $5 \mu\text{m}$). Whereas the tip emission is red-shifted at 300 K (a), it occurs at the same wavelength as the bulk at 4 K (b). At 300 K, excitons are more mobile and waveguiding is impeded due to an increased overlap between absorption and emission. At 4 K, waveguiding to the tip dominates. (c) At 300 K, the tip emission (red) matches the PL from a small PTCDI aggregate (green, note residual monomer emission at 540 nm) and is red-shifted with respect to the bulk wire (black), indicating exciton diffusion to a lower energy site formed at the tip. (d) At 4 K, the tip emission is identical to the bulk, suggesting that part of the bulk PL emerges from the tip without a loss in energy, that is, due to waveguiding. (e) Exciton migration to the tip is also evident in the PL dynamics of the tip versus the bulk due to a delayed rise and increased decay time of the tip PL at 300 K. (f) Tip-to-body PL intensity ratio for one single wire as a function of temperature. Typically, the tip brightens over 10-fold with respect to the body.

temperature, these regions are averaged out as the exciton energy exceeds the localization energy. Concomitantly, a quenching site will take up excitons from a larger volume, leading to a screening of the spatial intensity modulations.

Molecular aggregate nanowires have previously been found to support waveguiding of incident and emitted radiation.^{2,16,22–25} Given the fact that the intrinsic exciton lifetime is enhanced with respect to the monomer and excitons are quenched by thermally activated migration, it is crucial to differentiate between classical waveguiding and long-range exciton diffusion.¹³ Figure 2 shows spatially resolved emission spectra of a single wire at 300 K (a) and 4 K (b) under wide-field excitation with the wire PL microscope image inset. In all cases, the wire tip appears brighter than the bulk. At 300 K, the tip emission spectrum is shifted to the red with respect to the bulk (panel c), whereas it is indistinguishable at 4 K (d). We find that the 300 K tip spectrum matches the emission of small aggregates (panel c); as expected,³ smaller aggregates show stronger coupling and thus larger splitting between bright and dark states, leading to a red-shifted emission. Time-resolved PL recorded from the bulk and tip of a single wire at 300 K (panel e) generally exhibits a delayed onset and a longer lifetime of the tip PL with respect to the wire body. We propose that the red-shifted tip emission arises from exciton migration from the bulk wire to the tip, which in turn is comprised of a

smaller aggregate exhibiting lower-energy PL. Because of a significant overlap of the absorption and emission spectra, waveguiding is less pronounced at 300 K. As the temperature is lowered, exciton migration is inhibited due to disorder localization.³ At the same time, the PL spectrum narrows upon cooling, so that reabsorption of emitted light along the wire is reduced and waveguiding is enhanced. Consequently, the tips appear to brighten with respect to the bulk with a lowering of temperature, as exemplified by the single-wire tip-to-body brightness ratio in panel f.

The electronic structure of the aggregate is extremely sensitive to local packing of the molecules.¹⁶ A small topological defect in the crystal can form an effective quenching site for mobile excitons. It is possible to induce such a defect by mechanical force; some perylene aggregates even exhibit bulk “piezochromic” reversible transitions between J- and H-aggregates.²⁶ To confirm the occurrence of efficient exciton migration at room temperature, we created small defects in the crystal by nanoindentation using an AFM, as sketched in Figure 3a. An AFM tip ($\sim 15 \text{ nm}$ diameter) exerts a force of up to tens of nanonewtons on the top of a nanowire. Subsequently, fluorescence is excited and collected from below using a high numerical-aperture (1.4) objective lens and confocal detection. Prior to indentation, both the topography (panel b) and the PL (panel c) images appear uniform. Indentation

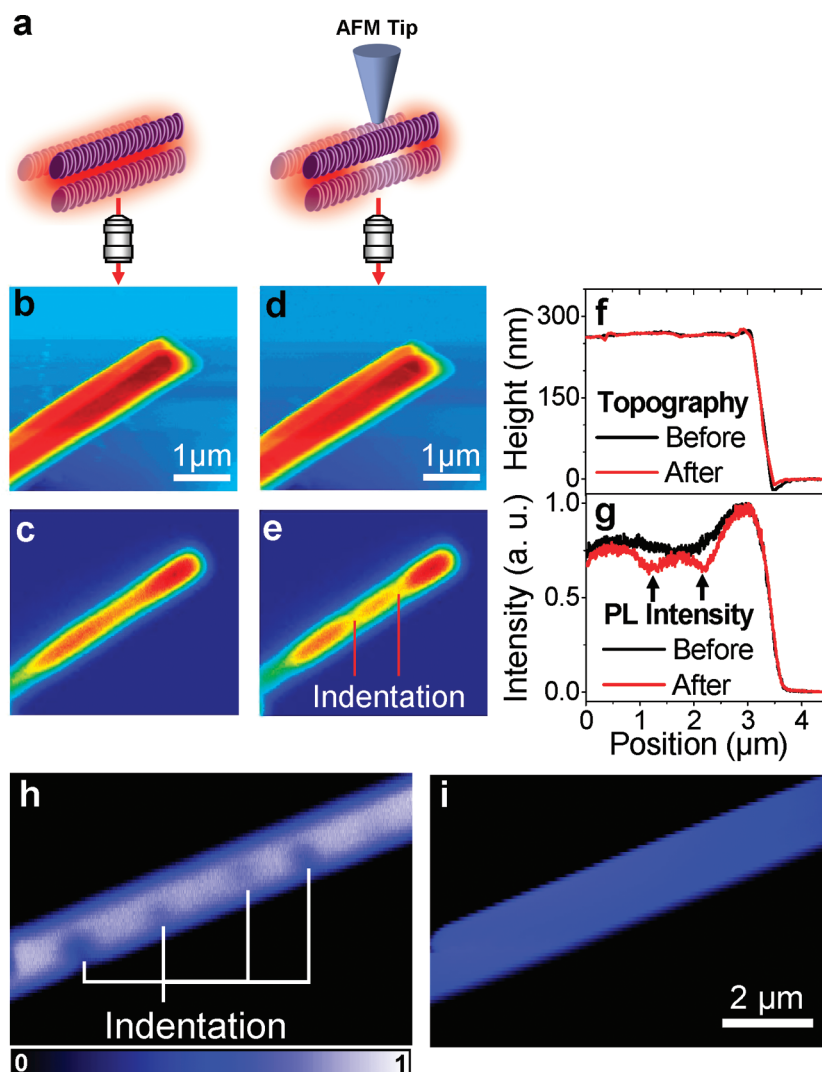


Figure 3. Nanomechanical modification of single wire PL at room temperature. In contact mode, the AFM tip is pressed into the top of the wire, and the PL is collected in a confocal scanning microscope from underneath following indentation. (a) Pressing on the nanowire with an AFM tip irreversibly forms a less emissive site. (b–e) Topographic (tapping mode) and PL images of a single wire before (b,c) and after (d,e) indentation. No change in the topography is discernible in the trace in (f), whereas a clear PL quenching is visible at the two positions of indentation (g). (h,i) Example of a “nanobarcode” written into a single wire. The indentation is only visible in PL (h), not in topography (i). From left to right, the extent of PL quenching at the sites of indentation is 35, 11, 6, and 20%, respectively.

does not modify the topography image (d), confirming that there is no irreversible damage to the wire. However, two permanent dark spots appear in the PL image at the locations of indentation (e). The AFM height trace (f) and PL intensity trace along the wire (g) before (black) and after (red) indentation substantiate these observations. Evidently, a small perturbation of the crystal surface, which does not alter the gross wire topography, is able to quench excitons that diffuse into its vicinity. In addition, indentation occurs over an area of only $\sim 200 \text{ nm}^2$, whereas the quenching is observed from a region as large as the diffraction limited spot ($\sim 1 \mu\text{m}$). The fact that the structural perturbation shows up in far-field PL imaging can only be explained by efficient exciton migration along the wire axis on a length scale of $>250 \text{ nm}$.²⁷ In absence of such a long-range exciton migration, one would expect the quenching to be very local (over a few nm), and therefore immeasurably small in far-field imaging. This was confirmed in a control experiment on a $\sim 200 \text{ nm}$ thick film of the conjugated polymer MEH-PPV, where no PL

quenching was observed upon nanoindentation due to a much shorter exciton diffusion length.

It is possible to estimate the exciton diffusion constant (D) provided one knows the exciton lifetime of the particular wire on which the quenching experiment is performed. Though a simultaneous measurement of PL lifetime and AFM quenching is not possible in our setup, one can still formulate a lower limit for D by assuming that the longest-lived excitons migrate the most. An exciton lifetime of 15 ns ²¹ and a diffusion length of 250 nm translates to a three-dimensional diffusion constant of $1.4 \times 10^{-2} \text{ cm}^2/\text{s}$; roughly 1–2 orders of magnitude higher than that characteristic of typical conjugated polymers.²⁸ Such a large value of D in these disordered molecular wires is all the more remarkable in light of a recent study on disorder-free single crystalline rubrene,²⁹ which reports an exciton diffusion constant of $0.25 \text{ cm}^2/\text{s}$. As a quenching mechanism, we propose that the AFM tip distorts the crystal surface slightly by reducing the rotational displacement

between the PTCDI molecules, in analogy to the bulk piezochromic effect reported previously.²⁶ The resulting local aggregates show more perfect H-aggregation and thus lower-energy excited states (E_1) and strongly forbidden transitions, enabling them to act as quenchers for neighboring excitons.

Besides demonstrating the occurrence of such surprisingly long-range exciton migration, nanoindentation of the aggregate offers a new way of encoding optical information in nanostructures by writing “nanobarcodes” as illustrated in Figure 3e,h. As fluorescent wires can be used in chemical sensing,³⁰ and potentially for energy conversion,³¹ it may be possible to write actual excitonic circuits into the wire structure using this nanoindentation approach. Ultimately, H-aggregate wires could be used to perform optical logic operations by means of controlled spatial shuttling and manipulation of excitons (such as by electric fields).³² In contrast to inorganic excitonic circuits,³³ such molecular materials would work at room temperature and allow facile programming by nanoscale force-induced structural modifications.

■ ASSOCIATED CONTENT

S **Supporting Information.** Sample preparation and experimental conditions are provided. This material is available free of charge via the Internet at <http://pubs.acs.org>.

■ AUTHOR INFORMATION

Corresponding Author

*E-mail: (D.C.) debangshuc@gmail.com; (J.M.L.) lupton@physics.utah.edu.

■ ACKNOWLEDGMENT

The authors are indebted to the following funding agencies for support: the David & Lucile Packard Fellowship and the Volkswagen Foundation (J.M.L., award no. I/84063), the NSF-DBI CAREER program (J.M.G., award no. 0845193), and NSF-CHE CAREER program (L.Z., award no. 0641353).

■ REFERENCES

- (1) Zang, L.; Che, Y. K.; Moore, J. S. *Acc. Chem. Res.* **2008**, *41*, 1596–1608.
- (2) Zhao, Y. S.; Fu, H.; Peng, A.; Ma, Y.; Liao, Q.; Yao, J. *Acc. Chem. Res.* **2010**, *43*, 409–418.
- (3) Pope, M.; Swenberg, C. E. *Electronic Processes in Organic Crystals and Polymers*; Oxford University Press: New York, 1999.
- (4) Balakrishnan, K.; Datar, A.; Naddo, T.; Huang, J.; Oitker, R.; Yen, M.; Zhao, J.; Zang, L. *J. Am. Chem. Soc.* **2006**, *128*, 7390–7398.
- (5) Lin, H.; Camacho, R.; Tian, Y.; Kaiser, T. E.; Würthner, F.; Scheblykin, I. G. *Nano Lett.* **2010**, *10*, 620–626.
- (6) Eisele, D. M.; Knoester, J.; Kirstein, S.; Rabe, J. P.; Vanden Bout, D. A. *Nat. Nanotechnol.* **2009**, *4*, 658–663.
- (7) Lagoudakis, P. G.; De Souza, M. M.; Schindler, F.; Lupton, J. M.; Feldmann, J.; Wenus, J.; Lidzey, D. G. *Phys. Rev. Lett.* **2004**, *93*, No. 257401.
- (8) Meinardi, F.; Cerminara, M.; Sassella, A.; Bonifacio, R.; Tubino, R. *Phys. Rev. Lett.* **2003**, *91*, No. 247401.
- (9) Köhler, A.; Bäessler, H. *Mater. Sci. Eng., R* **2009**, *R66*, 71–109.
- (10) Rocke, C.; Zimmermann, S.; Wixforth, A.; Kotthaus, J. P.; Böhm, G.; Weimann, G. *Phys. Rev. Lett.* **1997**, *78*, 4099–4102.
- (11) Priller, H.; Decker, M.; Hauschild, R.; Kalt, H.; Klingshirm, C. *Appl. Phys. Lett.* **2005**, *86*, No. 111909.
- (12) Scully, S. R.; Armstrong, P. B.; Edder, C.; Frechet, J. M. J.; McGehee, M. D. *Adv. Mater.* **2007**, *19*, 2961–2965.

- (13) Calzaferri, G.; Huber, S.; Maas, H.; Minkowski, C. *Angew. Chem., Int. Ed.* **2003**, *42*, 3732–3758.
- (14) Schlicke, B.; Belser, P.; De Cola, L.; Sabbioni, E.; Balzani, V. *J. Am. Chem. Soc.* **1999**, *121*, 4207–4214.
- (15) Guillet, T.; Berrehar, J.; Grousson, R.; Kovensky, J.; L-Mayer, C.; Schott, M.; Voliotis, V. *Phys. Rev. Lett.* **2001**, *87*, No. 087401.
- (16) Che, Y. K.; Yang, X. M.; Balakrishnan, K.; Zuo, J. M.; Zang, L. *Chem. Mater.* **2009**, *21*, 2930–2934.
- (17) Giaimo, J. M.; Lockard, J. V.; Sinks, L. E.; Scott, A. M.; Wislon, T. M.; Wasielewski, M. R. *J. Phys. Chem. A* **2008**, *112*, 2322–2330.
- (18) Gierschner, J.; Mack, H. G.; Oelkrug, D.; Waldner, I.; Rau, H. *J. Phys. Chem. A* **2004**, *108*, 257–263.
- (19) Würthner, F.; Chen, Z. J.; Dehm, V.; Stepanenko, V. *Chem. Commun.* **2006**, 1188–1190.
- (20) Seibt, J.; Marquetand, P.; Engel, V.; Chen, Z.; Dehm, V.; Würthner, F. *Chem. Phys.* **2006**, *328*, 354–362.
- (21) Since each nanowire is unique in terms of how disordered it is, its PL lifetime at 300 K is also unique. We observe a wide variability in the exciton lifetime (2–15 ns) between different wires.
- (22) Takazawa, K.; Kitahama, Y.; Kimura, Y.; Kido, G. *Nano Lett.* **2005**, *5*, 1293–1296.
- (23) O’Carroll, D.; Lieberwirth, I.; Redmond, G. *Nat. Nano.* **2007**, *2*, 180–184.
- (24) Balzer, F.; Bordo, V. G.; Simonsen, A. C.; Rubahn, H. G. *Phys. Rev. B* **2003**, *67*, No. 115408.
- (25) Yanagi, H.; Ohara, T.; Morikawa, T. *Adv. Mater.* **2001**, *13*, 1452–1455.
- (26) Yagai, S.; Seki, T.; Karatsu, T.; Kitamura, A.; Würthner, F. *Angew. Chem., Int. Ed.* **2008**, *47*, 3367–3371.
- (27) For a tiny quencher ($\sim 10^{-6} \mu\text{m}^3$, assuming 15 nm AFM tip size) to cause a significant PL quenching ($\sim 35\%$) over a sample volume that is 4 orders of magnitude larger ($\sim 10^{-2} \mu\text{m}^3$) in size would require a majority of the excitons created in that volume to migrate to the quenching site, and decay nonradiatively.
- (28) Markov, D. E.; Tanase, C.; Blom, P. W. M.; Wildeman, J. *Phys. Rev. B* **2005**, *72*, No. 045217.
- (29) Najafov, H.; Lee, B.; Zhou, Q.; Feldman, L. C.; Podzorov, V. *Nat. Mater.* **2010**, *9*, 938–943.
- (30) Naddo, T.; Che, Y.; Zhang, W.; Balakrishnan, K.; Yang, X.; Yen, M.; Zhao, J.; Moore, J. S.; Zang, L. *J. Am. Chem. Soc.* **2007**, *129*, 6978–6979.
- (31) Wicklein, A.; Ghosh, S.; Sommer, M.; Würthner, F.; Thelakkat, M. *ACS Nano* **2009**, *3*, 1107–1114.
- (32) Becker, K.; Lupton, J. M.; Müller, J.; Rogach, A. L.; Talapin, D. V.; Weller, H.; Feldmann, J. *Nat. Mater.* **2006**, *5*, 777–781.
- (33) High, A. A.; Novitskaya, E. E.; Butov, L. V.; Hanson, M.; Gossard, A. C. *Science* **2008**, *321*, 229–231.